Internal Methyl Rotation in the CH Stretching Overtone Spectra of 2-, 3-, and 4-Methylpyridine

Zimei Rong and Henrik G. Kjaergaard*,†

Department of Chemistry, University of Otago, P.O. Box 56, Dunedin, New Zealand

Bryan R. Henry*

Department of Chemistry and Biochemistry, University of Guelph, Guelph, Ontario, N1G 2W1, Canada

Received: November 20, 2001

A nonadiabatic model is presented to simulate the methyl regions of the overtone spectra of 2-, 3-, and 4-methylpyridine. The model incorporates harmonically coupled anharmonic oscillator local modes for CH stretching and rigid rotors for methyl internal rotation. Parameters for the model come from a series of ab initio calculations. The methyl regions of the overtone spectra are complex because of coupling between CH stretching and methyl torsion. Moreover there are differences between the similar spectra of 3- and 4-methylpyridine on one hand and the spectrum of 2-methylpyridine on the other. The simulation is successful in reproducing the methyl band profiles and in accounting for the spectral differences. Differences in the methyl band profiles are ascribed to differences in symmetry and magnitude of the frequency, anharmonicity, and torsional barrier and to differences in their dependence on the torsional angle. The success of the model and its ability to accommodate arbitrary functional forms of the frequency, anharmonicity, torsional barrier, and dipole moment function suggests its general applicability for the analysis of overtone spectra in a wide variety of molecules.

Introduction

XH stretching overtone spectra can be successfully explained by the local mode model. The origins of the local mode model can be traced to early work by Ellis who introduced a CH anharmonic oscillator model to explain the CH stretching overtone spectra of benzene[1] before Morse published his anharmonic oscillator model.[2] The model in its present form was introduced by Hayward and Henry[4−6] and extended to include interoscillator coupling in the harmonically coupled anharmonic oscillator (HCAO) local mode model.[7,8] Despite its success,[9−11] a pure stretching model could not always completely explain such overtone spectra. Different types of motion such as bending, molecular rotation, and internal rotation were found to affect overtone spectra through coupling with the stretching mode. Both bend−stretch (Fermi resonance) and coupling between stretching and rotation (Coriolis resonance) have been reviewed by Halonen.[11] Darling and Dennison included stretch−stretch coupling in the normal mode picture.[12] In this paper, we are interested in the coupling between CH stretching and methyl internal rotation (torsion).

Torsional effects on CH stretching spectra were studied first by Sheppard and Woodman.[13] They pointed out the torsional angle dependence of the force constant on methyl group torsion. When a methyl group rotates the CH bond lengths change, and the bond length is directly related to the oscillator frequencies.[10,14] Coupling between CH stretching and methyl torsion is a consequence of this dependence of the CH oscillator frequency on torsional angle. Anastasakos and Wildman simulated the methyl regions of the CH stretching overtone spectra of toluene and the xylenes with a model that described CH stretching as an anharmonic oscillator but expanded in a harmonic basis and the methyl torsion in a rigid rotor basis.[15] They used a linear dipole moment function which was independent of the torsional angle. Subsequently, such a dipole moment function was shown to be insufficient for overtone intensity calculations.[16,17] Cavagnat et al. use a Morse oscillator−rigid rotor basis model within the adiabatic approximation and obtain good agreement between the observed and calculated spectra for the fundamental and overtone CH stretching regions of nitromethanes, toluenes, and methylpyridines.[18−22] Zhu et al. simulated the methyl region of the overtone spectrum of 2,6-difluorotoluene with a nonadiabatic model that included all three CH oscillators of the methyl group within the HCAO approximation and described methyl torsion in a rigid rotor basis.[23]

We have successfully reproduced the observed methyl band profiles in the CH stretching overtone spectra of toluene-d_0, -α-d_1, and -α-d_2.[24] Our model could account for changes in methyl profiles between the three molecules with different degrees of deuteration and confirmed the importance of coupling between methyl torsion and CH stretching motion.

In our recent work on the overtone spectra of *o*-, *m*-, and *p*-xylenes, we have generalized our model for toluene-d_0, toluene-α-d_1, and toluene-α-d_2, where there is a V_6 torsional barrier, to a model, which can accommodate molecules with barriers of arbitrary symmetry and arbitrary magnitude.[25] In our model, we approximated the torsional potential, frequency, and anharmonicity with a sixth-order Fourier series as a function of the torsional angle θ. The dipole moment functions were

† On sabbatical at Cooperative Institute for Research in Environmental Sciences (CIRES), University of Colorado, Boulder, CO 80309-0216.

10.1021/jp014300u CCC: $22.00
Published on Web 04/05/2002

approximated by a Taylor series for the stretching coordinate, and the Taylor series coefficients were approximated by a Fourier series in the torsional angle. Our model accommodated the potential, frequency, anharmonicity, and dipole moment function in arbitrary functional forms, and we will use it in this paper to simulate the methyl regions of the overtone spectra of 2-, 3-, and 4-methylpyridine.

The generalized model was successful in reproducing the methyl regions of the overtone spectra of *o*-, *m*-, and *p*-xylene.[25] The overtone spectra of *m*- and *p*-xylene with quasi-free methyl rotors are similar to the overtone spectra of toluene.[25] For molecules with a very low barrier to methyl torsion such as toluene and *m*- and *p*-xylene, the methyl group exists without a preferred conformation. The methyl overtone spectrum of *o*-xylene, which has a high torsional barrier of 460 cm^{-1}, is similar to the methyl overtone spectra of dimethyl ether and propane.[16,17] The methyl group of *o*-xylene exists in a single preferred conformation relative to the ring frame. The two conformationally distinct methyl CH bonds, out-of-plane and in-plane, differ in bond length. This bond length difference leads to a frequency difference of the CH oscillators that is reflected in two distinct peaks in the overtone spectrum. Our generalized simulation leads to the same result as this straightforward simple interpretation.[25]

Theoretically, our CH stretching methyl torsion model could be applied to any molecule. Practically, we have used the model successfully for lower barrier molecules such as *m*- and *p*-xylene, with barriers of 10 and 25 cm^{-1}, and the high barrier molecule *o*-xylene, with a barrier of 460 cm^{-1}.[25] Application to other molecules with different torsional barriers will verify the generality of our model. The methylpyridines have ab initio barrier heights of 85 cm^{-1} for 2-methylpyridine, 53 cm^{-1} for 3-methylpyridine, and 2 cm^{-1} for 4-methylpyridine and represent a useful series for this purpose.

Proos and Henry have recorded the room-temperature vapor phase overtone spectra of 2-, 3-, and 4-methylpyridine in the CH stretching region corresponding to $\Delta v_{CH} = 2-6$.[26] They analyzed the methyl regions of 2-, 3-, and 4-methylpyridine according to their barriers and concluded that vibrational torsional coupling is an important contributor to the complex methyl structure. They found that the change in barrier from the 6-fold 2-cm^{-1} barrier of 4-methylpyridine to the 3-fold 53-cm^{-1} barrier of 3-methylpyridine has little effect on the methyl band profile as the observed methyl band profiles of 3-methylpyridine are similar to those of 4-methylpyridine. However, the methyl band profiles change from 3-methylpyridine to 2-methylpyridine as the barrier size changes from 53 to 85 cm^{-1}.

Cavagnat et al. simulated methyl band profiles of methylpyridine-2-α-d_2 and methylpyridine-3-α-d_2 at $\Delta v_{CH} = 1-4$ and methylpyridine-4-α-d_2 at $\Delta v_{CH} = 1$.[21,22] Due to the deuteration, the CH stretching problem is limited to a single CH. They successfully reconstructed their experimental spectra for these molecules. They concluded that stretching torsional coupling is the origin of the complex methyl profiles and that the change in type and size of the torsional barrier is the origin of the significant spectral differences.

In this paper, we apply our CH stretching methyl torsion model to 2-, 3-, and 4-methylpyridine with their differing methyl torsional barriers. The methyl overtone spectrum of 2-methylpyridine is different from the overtone spectrum of either a low or high barrier molecule. We will analyze the methyl band differences in the three methylpyridines according to the frequencies, anharmonicities, and torsional barriers.

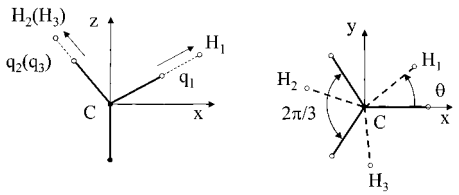

Figure 1. Coordinate system used to describe the rotating methyl group. The projection on the *xz* plane is shown on the left with a depiction of the CH stretching displacement coordinates, q_i. The figure on the right shows the projection on the *xy* plane. The methyl group depicted by the dashed lines has been rotated θ degrees from the minimum energy conformer shown with solid lines. The torsional angle $\theta_1 = \theta$, $\theta_2 = \theta + 2\pi/3$, and $\theta_3 = \theta - 2\pi/3$. The ring is in the *xz* plane.

Theory and Calculations

The theoretical model that we used for the intensity calculations is similar to the model that we used in our previous work on *o*-, *m*-, and *p*-xylene.[25] For completeness we give a brief description here. We use the oscillator strength f_{eg} of a vibrational transition from the ground state *g* to a vibrationally excited state *e* as a measure of intensity. Oscillator strength is given by the expression[17,27]

$$f_{eg} = 4.702 \times 10^{-7}[\text{cm D}^{-2}]\tilde{\nu}_{eg}|\vec{\mu}_{eg}|^2 \qquad (1)$$

where $\tilde{\nu}_{eg}$ is the vibrational transition frequency in cm^{-1} and $\vec{\mu}_{eg} = \langle e|\vec{\mu}|g\rangle$ is the transition dipole moment in debye (D). The vibrational wave functions and energies of the methyl group are obtained with the CH stretching methyl torsion model, which describes CH stretching within the harmonically coupled anharmonic oscillator local mode model and internal rotation in a rigid rotor basis. The dipole moment functions are obtained from a series of ab initio calculations. The dipole moment functions of the methyl group are expanded in internal CH displacement coordinates q_i and the torsional angle θ.

Methyl Coordinate System. The choice of coordinates for the three methyl CH bonds is shown in Figure 1 (see also ref 25). The Hamiltonian and the dipole moment function of the methyl group, including both CH stretching and methyl torsion, are described within this coordinate system. The coordinate system is fixed to the ring frame. The *z* axis contains the C−C bond around which the methyl group rotates, and the positive *z*-direction is from the carbon atom on the ring toward the methyl carbon atom. The *x*-axis is in the plane of the ring (*xz* plane). The positive *x*-axis direction is toward the first hydrogen atom (H_1) and the *y*-axis is perpendicular to the ring plane. In 2- and 3-methylpyridine the nitrogen atom is at positive *x*. The hydrogen atom at positive *y* is numbered as the second hydrogen atom (H_2). The projections of the methyl group on the *xz* and *xy* planes are illustrated on the left and right sides of Figure 1, respectively. The methyl torsional angle, $\theta = \theta_1$, is defined as the dihedral angle between the plane consisting of the first CH_1 bond and the *z*-axis and the *xz* plane. The positive torsional angle is defined from the positive *x*-axis toward the positive *y*-axis. Torsional angles for the other two CH bonds are $\theta_2 = \theta_1 + 2\pi/3$ and $\theta_3 = \theta_1 - 2\pi/3$.

Methyl Hamiltonian. The functional forms of potential, frequency and anharmonicity are approximated as Fourier series limited to the sixth order. This leads to a total of 13 terms for each quantity and we express these in terms of a column vector $F_i = [1, \cos(\theta_i), ..., \cos(6\theta_i), \sin(\theta_i), ..., \sin(6\theta_i)]^T$ with

a dimension of 13. The total Hamiltonian for a rotating methyl group is given by[25]

$$H_{v_1v_2v_3}/hc = \sum_{i=1}^{3}\left[\Omega F_i\left(v_i+\frac{1}{2}\right) - XF_i\left(v_i+\frac{1}{2}\right)^2\right] + VF_1 + Bm^2 - \gamma'(a_1a_2^{+} + a_1^{+}a_2 + a_2a_3^{+} + a_2^{+}a_3 + a_3a_1^{+} + a_3^{+}a_1) \quad (2)$$

where Ω and X are the Fourier series expansion coefficients for the frequency and anharmonicity. The torsional potential is VF_1. The indices refer to the three methyl CH_i bonds and torsional angles θ_i, which are defined in Figure 1. γ' is the effective CH stretch−stretch coupling constant.[17,28] The small variation of γ' with θ is ignored. a and a^+ are the step up and step down operators of harmonic oscillators. B is the rotational constant for the methyl group. We do not include the small variation in B with torsional angle and vibrational excitation.

Methyl Dipole Moment Function. The methyl dipole moment function is approximated by a series expansion in the CH stretching coordinates and the torsional angle. The expansion is written in a matrix form similar to the Hamiltonian. The permanent dipole moment is omitted since it does not contribute to the vibrational transition intensities. Thus the x component of the dipole moment vector becomes

$$\mu_x = \sum_{i=1}^{3} Q_i C_x F_i \quad (3)$$

where $Q_1 = [q_1, q_1^2, q_1^3, q_1^4, q_1^5, q_1^6, q_2q_3, q_2^2q_3, q_2q_3^2]$. The Q_2 and Q_3 vectors are obtained from Q_1 by permutation of the appropriate indices. The Fourier series column vectors F_i were defined previously. The dipole moment function expansion coefficients are evaluated by ab initio calculations and are tabulated in the 9×13 matrix C_x. The y and z components of the dipole moment vector are obtained in a similar fashion with expansion coefficient matrixes C_y and C_z, respectively.

Ab Initio Calculations. The coefficient matrixes Ω, X, V, C_x, C_y, and C_z are obtained from a series of ab initio calculations. The ab initio calculations can be divided into two parts. Initially, at each torsional position, we change the CH_1 oscillator bond length from −0.3 to 0.4 Å with a 0.05 Å increment and calculate a 15-point grid of ab initio dipole moments. These 15 grid points are fitted with a sixth-order least-squares fit to obtain the Taylor series expansion coefficients. We calculate the potential energy at 9 points from −0.2 to 0.2 Å to obtain the second- and third-order energy derivative coefficients from a sixth-order least-squares fit. From these energy derivatives we calculate the frequency and anharmonicity. We repeat all of these calculations for each 10-deg rotation of the methyl group from 0° to 180°. For each torsional angle, the molecular geometry is fully optimized with a fixed torsional angle before the CH_1 stretching grid is calculated. The angular dependence of the frequency, anharmonicity, and dipole moment function Taylor expansion coefficients is described by fitting each in turn to a sixth-order Fourier series with a MATLAB least-squares fitting program.[29]

The overtone intensities are less sensitive to the mixed dipole moment function Taylor expansion coefficients. For the torsional angles of 0°, 90°, and 180°, a two-dimensional 5×5 grid with a 0.05-Å step size is calculated.[16,17,28] The dipole moment Taylor expansion coefficients for the q_1q_2, $q_1q_2^2$, and $q_1^2q_2$ terms and the mixed force constant are determined from these two-dimensional grids with a third-order least-squares fit. At torsional angles of 0° and 180° a symmetric grid is used, whereas an asymmetric grid is needed for 90°. The Fourier series coefficients for the Taylor series coefficients are obtained by solving a system of linear equations. The mixed force constant is used to calculate the effective coupling coefficient. All grid points and the optimized geometries are calculated with Gaussian 94.[30] We use the Hartree−Fock (HF) level of theory and the 6-31G(d) basis set in all ab initio calculations.

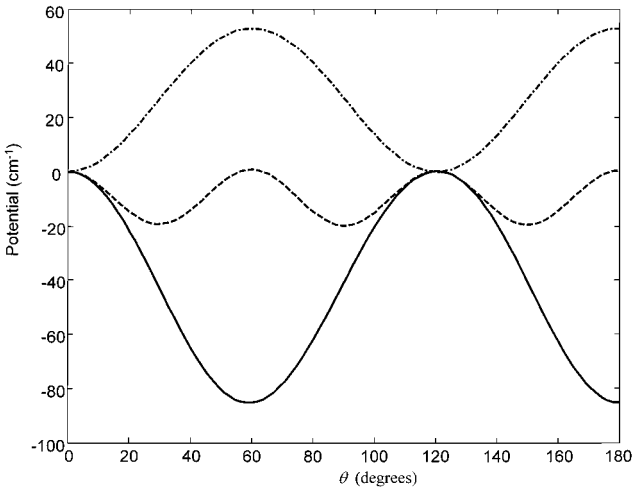

Figure 2. Torsional potentials of 2-methylpyridine (—), 3-methylpyridine (- · -), and 4-methylpyridine (- - -) as a function of the torsional angle, θ. The potential of 4-methylpyridine is multiplied by 10 for clarity.

Results and Discussion

The ab initio potentials of 2-, 3-, and 4-methylpyridine as functions of torsional angle are shown in Figure 2. We define the torsional angle to be zero when the CH_1 bond is in the ring plane and toward the nitrogen atom for 2- and 3-methylpyridine. The minimum energy in 3-methylpyridine occurs at a torsional angle of zero (the in-plane methyl H atom faces the nitrogen atom).[21,26] The minimum energy in 2-methylpyridine occurs at a torsional angle of 60° (the in-plane methyl H atom is opposite the nitrogen atom).[21,26] It is interesting to note that when the methyl group is in close proximity to the nitrogen atom in 2-methylpyridine, the in-plane hydrogen is opposite the nitrogen at the minimum energy conformer. When the methyl group is further away from the nitrogen atom in 3-methylpyridine, the in-plane hydrogen is toward the nitrogen at the minimum energy conformer. The 2-methylpyridine minimum energy conformation is dictated by an attractive nonbonded interaction between the methyl hydrogen and the lone pair on the adjacent nitrogen. The nitrogen lone pair is not involved in ring aromaticity and occupies an orbital lying in the ring plane. Lone pairs occupy more space than bond pairs. Thus it is reasonable that the sum of the attractive interactions between the lone pair and the two hydrogens in the methyl CH bonds at 60° exceeds the attractive interaction that would occur for a single planar methyl CH bond directly adjacent to the nitrogen. The minimum energy in 4-methylpyridine occurs at a torsional angle of 30° (one CH bond of the methyl rotor is perpendicular to the ring plane).[22,26]

The experimental and calculated torsional potential expansion coefficients of 2-, 3-, and 4-methylpyridine are given in Table 1.[31,32] The calculated potentials of 2- and 4-methylpyridine are in good agreement with the experimental ones. 4-Methylpyridine has a small 6-fold barrier as expected, which is similar to toluene and to *m*- and *p*-xylene.[24,25] 2- and 3-Methylpyridine both have significant 3-fold barriers. The barrier in *o*-xylene is also 3-fold but is more than 4 times higher than in 2-methylpyridine.[25]

TABLE 1: Potential, Frequency, and Anharmonicity as a Function of Torsional Angle for 2-, 3-, and 4-Methylpyridine[a]

molecule	parameter	1	cos(θ)	cos(2θ)	cos(3θ)	cos(4θ)	cos(5θ)	cos(6θ)
2-methylpyridine	exptl V[b]	47.3			45.2			−2.1
	calcd V[c]	45.7	−0.9	−0.4	42.7	0.4	0.8	−0.5
	calcd Ω[c,e]	3067.9	17.1	25.1	−0.1	−1.4	0.2	0.0
	calcd X[c,e]	59.3	−0.4	−0.6	0.0	0.0	0.0	0.0
3-methylpyridine	exptl V[d]							
	calcd V[c]	26.9	0.1	0.0	−26.4	0.0	−0.1	−0.3
	calcd Ω[c,e]	3056.6	1.2	17.1	−0.3	−1.0	0.1	0.0
	calcd X[c,e]	59.7	−0.1	−0.5	0.0	0.0	0.0	0.0
4-methylpyridine	exptl V[b]	2.4						2.4
	calcd V[c]	1.0	0.0	0.0	0.0	0.0	0.0	1.0
	calcd Ω[c,e]	3062.6	−0.2	17.4	0.0	−0.9	0.2	0.0
	calcd X[c,e]	59.5	0.0	−0.4	0.0	0.0	0.0	0.0

[a] The sixth-order Fourier series expansion coefficients of the potential (V), frequency (Ω), and anharmonicity (X) in cm^{-1}. [b] The experimental potentials of 2-methylpyridine in ref 30 and 4-methylpyridine in ref 31 have been converted from the conventional form $(V_{3n}/2)[1 - \cos(3n\theta)]$ to the Fourier series. [c] Calculated with the HF/6-31G(d) method. [d] Experimental value is not available. [e] The calculated frequencies and anharmonicities have been scaled with the scaling factors of 0.9377 and 0.907, respectively.

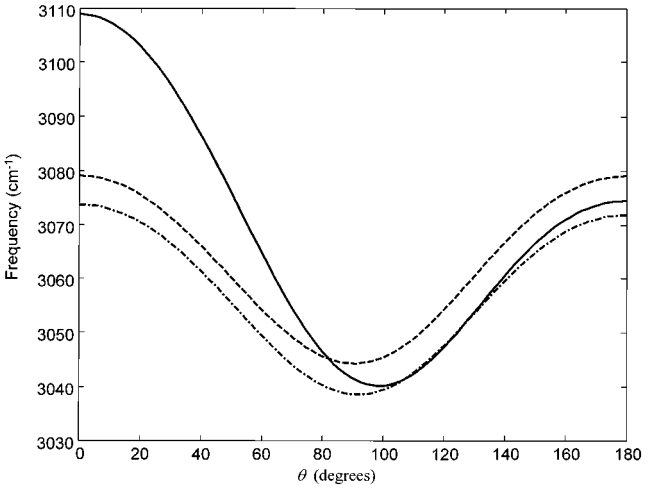

Figure 3. Methyl CH stretching frequencies of 2-methylpyridine (—), 3-methylpyridine (- · -), and 4-methylpyridine (- - -) as a function of the torsional angle, θ.

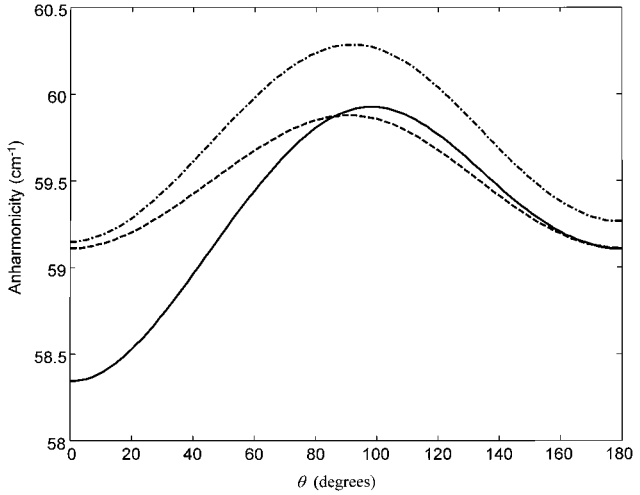

Figure 4. Methyl diagonal CH stretching anharmonicities of 2-methylpyridine (—), 3-methylpyridine (- · -), and 4-methylpyridine (- - -) as a function of the torsional angle, θ.

The methyl regions of the overtone spectra of 3- and 4-methylpyridine are similar but differ from the methyl regions of the overtone spectrum of 2-methylpyridine (see Figures 1−5 of ref 26). The methyl torsional potentials of 2-, 3-, and 4-methylpyridine differ from each other in form, symmetry, and magnitude (Figure 2). Differences in magnitude between the potentials of 3- and 4-methylpyridine are similar to the corresponding differences between 2- and 3-methylpyridine. However, the only significant spectral differences occur between 3- and 4-methylpyridine on one hand and 2-methylpyridine on the other. Thus, it is unlikely that an explanation of spectral differences will be found solely from the torsional potential.

The local mode frequency and anharmonicity expansion coefficients of 2-, 3-, and 4-methylpyridine are listed in Table 1. The frequencies of 2-, 3-, and 4-methylpyridine as functions of the torsional angle are shown in Figure 3 and the anharmonicities in Figure 4. The angular dependences of the frequencies and anharmonicities of 3- and 4-methylpyridine are very close to a constant plus cos(2θ) term. The angular dependence of the frequency and anharmonicity of 2-methylpyridine is more complex as can be seen from Figures 3 and 4. The values in Table 1 indicate that the cos(θ) terms are significant for both the frequency and anharmonicity of 2-methylpyridine. All sin($m\theta$) terms in the expansions, where m is an integer, disappear due to the planar symmetry of the ring frame. The frequency dependence on θ arises because of a weakening of the CH σ bonds when they are out of the plane of the aromatic ring. The in-plane methyl CH is shorter than the two at 60°. Ab initio calculations show an increase in antibonding character for the out of plane CH bonds due to interaction with the π molecular orbitals on the aromatic ring. Such an interaction vanishes for the in-plane methyl CH bond.

The methyl band overtone spectrum of 2-methylpyridine is slightly blue-shifted as compared to the 3- and 4-methylpyridine spectra (see Figures 1−5 in ref 26). This blue shift is a consequence of a higher mean frequency and lower mean anharmonicity in 2-methylpyridine as compared to 3- and 4-methylpyridine (see Figures 3 and 4).

Differences in the methyl band profiles of 3- and 4-methylpyridine as compared to 2-methylpyridine arise from differences in the angular dependence of frequency and anharmonicity. The frequency changes $\delta\omega$ and anharmonicity changes $\delta\omega x$ for 3- and 4-methylpyridine are similar to each other but are not similar to the changes for 2-methylpyridine. The frequency and anharmonicity deviation have effects on the Hamiltonian that depend on v, the vibrational quantum number $[(v + 1/2)\delta\omega - (v + 1/2)^2\delta\omega x]$, whereas the potential term V in the methyl Hamiltonian is independent of v. The slight differences in the methyl band overtone spectra of 3- and 4-methylpyridine are caused by the barrier height. The torsional barrier difference between 2- and 3-methylpyridine is overshadowed by differences in the angular dependence of frequency and anharmonicity, which lead to the significant differences in methyl band profiles (vide infra).

TABLE 2: Ab Initio HF/6-31(d) Dipole Moment Expansion Coefficients for Methyl Stretching and Torsion of 2-Methylpyridine[a]

C_x	units	1	cos(θ)	cos(2θ)	cos(3θ)	cos(4θ)	cos(5θ)	cos(6θ)	sin(θ)
q_1	D/Å	0.053	−0.517	0.077	0.005	0.005	0.001	0.000	
q_1^2	D/Å^2	0.007	−0.963	0.048	0.027	0.004	−0.002	0.000	
q_1^3	D/Å^3	−0.007	0.230	−0.010	0.032	0.001	0.000	0.000	
q_1^4	D/Å^4	−0.007	−0.176	−0.017	−0.035	0.000	0.002	0.000	
q_1^5	D/Å^5	0.002	0.231	−0.004	−0.030	−0.002	0.001	0.000	
q_1^6	D/Å^6	0.008	−0.028	0.014	0.033	−0.001	0.001	0.000	
q_2q_3[b]	D/Å^2	0.028	−0.307	−0.026					
$q_2q_3^2$[b]	D/Å^3	0.003	−0.011						0.259
$q_2^2q_3$[b]	D/Å^3	0.003	−0.011						−0.208
C_y	units	1	cos(θ)	sin(θ)	sin(2θ)	sin(3θ)	sin(4θ)	sin(5θ)	sin(6θ)
q_1	D/Å			−0.604	0.050	0.009	0.004	0.000	0.000
q_1^2	D/Å^2			−1.135	0.031	0.021	0.002	−0.002	0.000
q_1^3	D/Å^3			0.277	−0.004	0.027	0.001	0.000	0.000
q_1^4	D/Å^4			−0.183	−0.009	−0.033	0.000	0.001	0.000
q_1^5	D/Å^5			0.234	−0.009	−0.024	−0.002	0.001	0.000
q_1^6	D/Å^6			0.018	0.008	0.034	−0.001	0.001	0.000
q_2q_3[b]	D/Å^2			−0.287	0.000				
$q_2q_3^2$[b]	D/Å^3	0.010	0.213	−0.059					
$q_2^2q_3$[b]	D/Å^3	−0.010	−0.213	0.004					
C_z	units	1	cos(θ)	cos(2θ)	cos(3θ)	cos(4θ)	cos(5θ)	cos(6θ)	sin(θ)
q_1	D/Å	−0.458	0.058	−0.013	0.003	−0.006	−0.001	0.000	
q_1^2	D/Å^2	−0.809	0.049	0.131	0.004	−0.005	0.002	0.000	
q_1^3	D/Å^3	0.010	−0.004	0.111	0.000	0.010	0.002	−0.001	
q_1^4	D/Å^4	0.141	−0.003	−0.004	−0.006	0.007	0.001	−0.002	
q_1^5	D/Å^5	0.087	−0.006	−0.014	−0.005	0.000	0.000	0.001	
q_1^6	D/Å^6	0.017	−0.002	−0.093	0.003	−0.001	−0.003	0.003	
q_2q_3[b]	D/Å^2	0.363	0.020	0.086					
$q_2q_3^2$[b]	D/Å^3	0.060	−0.001						−0.004
$q_2^2q_3$[b]	D/Å^3	0.060	−0.001						0.030

[a] The dipole moment function is expanded in the CH stretching coordinate as a Taylor series and the torsional coordinate in a Fourier series. The terms that are zero by symmetry have been left out. For the *x* and *z* components, the sin($m\theta$) diagonal and second-order mixed stretching terms are zero. For the *y* component, the cos($m\theta$) diagonal and second-order mixed stretching terms are zero. [b] Fourier expansion is limited (see text).

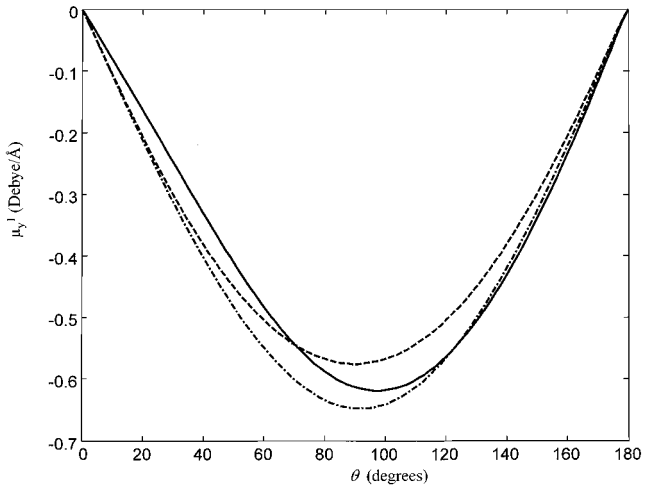

Figure 5. First-order dipole moment displacement expansion coefficients of the *y* component in 2-methylpyridine (—), 3-methylpyridine (- • -), and 4-methylpyridine (- - -) versus the torsional angle, θ.

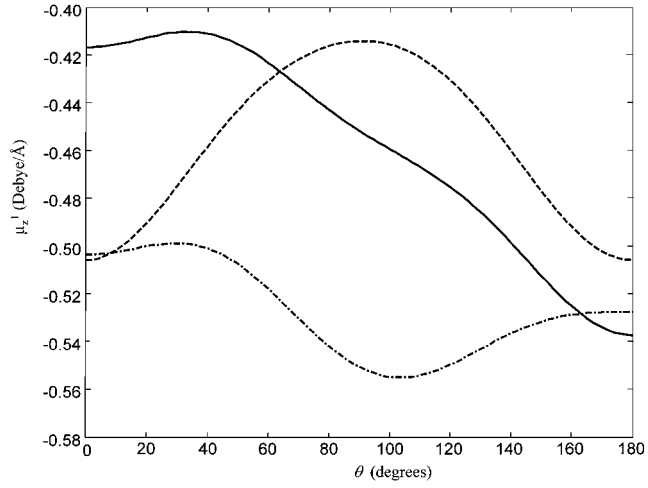

Figure 6. First-order dipole moment displacement expansion coefficients of the *z* component in 2-methylpyridine (—), 3-methylpyridine (- • -), and 4-methylpyridine (- - -) versus the torsional angle, θ.

The expansion coefficients of the dipole moment function of 2-, 3-, and 4-methylpyridine are given in Tables 2−4. The angular dependences of the first-order CH_1 displacement expansion coefficients of the *y* and *z* component are shown in Figures 5 and 6, respectively, and the angular dependences of the second-order CH_1 displacement expansion coefficients of the *z* component is shown in Figure 7. Due to the planar symmetry of the ring, the C_x and C_z coefficients have zero sin($m\theta$) components for the diagonal and second-order mixed terms, whereas C_y has only sin($m\theta$) components. The mixed dipole expansion terms are less important and are limited to fewer Fourier expansion terms.

The dipole moment function expansion coefficients are similar for the three methylpyridines. From a chemical point of view such results are to be expected. In both toluene and the isoelectronic methylpyridines, a methyl group is attached to an aromatic ring through a carbon−carbon σ bond lying in the ring plane. The dipole moment derivatives reflect changes in the

TABLE 3: Ab Initio HF/6-31(d) Dipole Moment Expansion Coefficients for Methyl Stretching and Torsion of 3-Methylpyridine[a]

C_x	units	1	cos(θ)	cos(2θ)	cos(3θ)	cos(4θ)	cos(5θ)	cos(6θ)	sin(θ)
q_1	D/Å	0.008	−0.583	0.003	−0.009	0.000	−0.001	0.000	
q_1^2	D/Å^2	0.007	−1.013	0.002	0.026	0.000	−0.002	0.000	
q_1^3	D/Å^3	0.008	0.228	0.002	0.040	0.000	0.001	0.000	
q_1^4	D/Å^4	−0.007	−0.154	0.000	−0.023	0.000	0.003	0.000	
q_1^5	D/Å^5	0.003	0.223	−0.003	−0.028	0.000	0.002	0.000	
q_1^6	D/Å^6	−0.004	−0.027	0.002	0.022	0.000	−0.001	0.000	
q_2q_3[b]	D/Å^2	0.001	−0.317	−0.006					
$q_2q_3^2$[b]	D/Å^3	0.001	−0.008						0.229
$q_2^2q_3$[b]	D/Å^3	0.001	−0.008						−0.227
C_y	units	1	cos(θ)	sin(θ)	sin(2θ)	sin(3θ)	sin(4θ)	sin(5θ)	sin(6θ)
q_1	D/Å			−0.644	0.009	0.003	0.000	0.000	0.000
q_1^2	D/Å^2			−1.200	0.008	0.022	−0.001	−0.001	0.000
q_1^3	D/Å^3			0.261	0.002	0.031	0.000	0.001	0.000
q_1^4	D/Å^4			−0.164	−0.003	−0.022	0.001	0.002	0.000
q_1^5	D/Å^5			0.238	−0.001	−0.022	0.000	0.003	0.000
q_1^6	D/Å^6			0.025	0.001	0.024	0.000	0.000	0.000
q_2q_3[b]	D/Å^2			−0.303	0.000				
$q_2q_3^2$[b]	D/Å^3	0.001	0.232	−0.019					
$q_2^2q_3$[b]	D/Å^3	−0.001	−0.232	0.100					
C_z	units	1	cos(θ)	cos(2θ)	cos(3θ)	cos(4θ)	cos(5θ)	cos(6θ)	sin(θ)
q_1	D/Å	−0.527	0.019	0.018	−0.007	−0.006	0.000	0.000	
q_1^2	D/Å^2	−0.872	0.016	0.179	−0.001	−0.005	0.000	0.000	
q_1^3	D/Å^3	−0.012	−0.003	0.113	0.002	0.009	0.000	−0.001	
q_1^4	D/Å^4	0.147	−0.003	−0.005	0.003	0.009	0.000	−0.001	
q_1^5	D/Å^5	0.080	−0.002	−0.011	0.001	0.006	0.000	0.001	
q_1^6	D/Å^6	0.057	0.002	−0.102	−0.001	0.000	0.000	0.003	
q_2q_3[b]	D/Å^2	0.397	0.002	0.100					
$q_2q_3^2$[b]	D/Å^3	0.071	0.000						0.002
$q_2^2q_3$[b]	D/Å^3	0.071	0.000						0.006

[a] The dipole moment function is expanded in the CH stretching coordinate as a Taylor series and the torsional coordinate in a Fourier series. The terms that are zero by symmetry have been left out. For the *x* and *z* components, the sin($m\theta$) diagonal and second-order mixed stretching terms are zero. For the *y* component, the cos($m\theta$) diagonal and second-order mixed stretching terms are zero. [b] Fourier expansion is limited (see text).

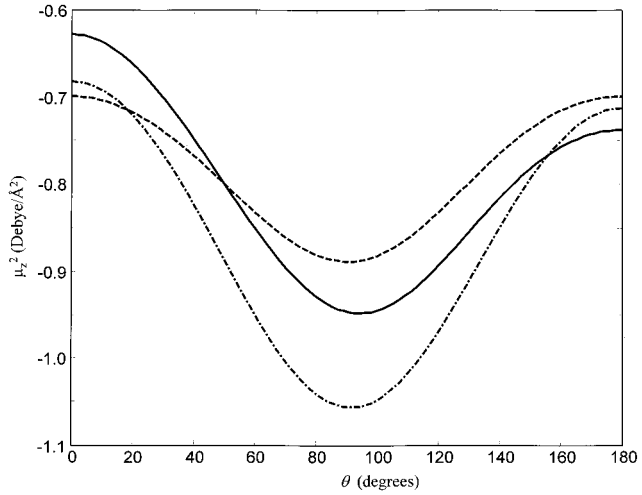

Figure 7. Second-order dipole moment displacement expansion coefficients of the *z* component in 2-methylpyridine (—), 3-methylpyridine (- • -), and 4-methylpyridine (- - -) versus the torsional angle, θ.

electronic environment of the CH methyl σ bond with CH bond length. Any such changes are unlikely to be affected by the position of the methyl substitution.

For 2-, 3-, and 4-methylpyridine, the C_z component is reasonably approximated by a constant plus cos(2θ) term, the C_x by a cos(θ) term, and the C_y by a sin(θ) term as we have shown previously for toluene.[33] This approximation is very good for 4-methylpyridine, becomes slightly less valid for 3-methylpyridine, and is worse again for 2-methylpyridine. Not all diagonal dipole moment expansion coefficients are affected equally. The first-order dipole moment expansion coefficients for 2-, 3-, and 4-methylpyridine in the y component are very similar to each other as seen in Figure 5, whereas those in the *z* component are dissimilar as seen in Figure 6. Thus differences in fundamental spectra are expected. However, overtone spectra are dominated by higher order terms in the dipole moment expansion. These are similar for the three methylpyridines. For example, Figure 7 shows the second-order derivative for the *z* component.

We calculate the methyl spectral profiles of the methylpyridines using the harmonically coupled anharmonic oscillator (HCAO) local mode model for CH stretching and a rigid rotor basis for the torsion. The simulation parameters (frequencies, anharmonicities, potentials in Table 1, and dipole moment functions in Tables 2−4) are calculated ab initio with the HF/6-31G(d) method. Calculated frequencies and anharmonicities are often overestimated, so scaling factors are usually used.[34] We have taken the scaling factors for the methylpyridines from the aryl peak of *p*-xylene.[25] The scaling factors are 0.9377 for the frequency and 0.907 for the anharmonicity, respectively.[35]

The rotational constants *B* for the methyl groups of 2-, 3-, and 4-methylpyridine are calculated to be 5.42, 5.45, and 5.44 cm^{-1}, respectively, for the optimized geometries with the HF/6-31G(d) method. The *B* values of the three molecules are very similar to each other and to the values found for *o*-, *m*-, and *p*-xylene.[25] The *B* value will decrease as the methyl CH oscillators are excited to higher CH stretching vibrational levels. They will have slight variations between the different vibrational states with the same total v and at different torsional angles.

TABLE 4: Ab Initio HF/6-31(d) Dipole Moment Expansion Coefficients for Methyl Stretching and Torsion of 4-Methylpyridine[a]

C_x	units	1	cos(θ)	cos(2θ)	cos(3θ)	cos(4θ)	cos(5θ)	cos(6θ)	sin(θ)
q_1	D/Å	0.000	−0.570	0.000	−0.010	0.000	0.000	0.000	
q_1^2	D/Å^2	0.000	−0.984	−0.001	0.008	0.001	−0.002	0.000	
q_1^3	D/Å^3	0.000	0.258	0.000	0.028	0.000	0.000	0.000	
q_1^4	D/Å^4	0.000	−0.158	0.000	−0.025	0.000	0.002	0.000	
q_1^5	D/Å^5	0.000	0.217	0.000	−0.026	0.000	0.002	0.000	
q_1^6	D/Å^6	0.000	−0.029	0.000	0.025	0.000	0.000	0.000	
q_2q_3[b]	D/Å^2	0.000	−0.306	0.000					
$q_2q_3^2$[b]	D/Å^3	0.000	−0.008						0.234
$q_2^2q_3$[b]	D/Å^3	0.000	−0.008						−0.234
C_y	units	1	cos(θ)	sin(θ)	sin(2θ)	sin(3θ)	sin(4θ)	sin(5θ)	sin(6θ)
q_1	D/Å			−0.583	0.000	−0.008	0.000	0.000	0.000
q_1^2	D/Å^2			−1.124	−0.001	0.005	−0.001	−0.002	0.000
q_1^3	D/Å^3			0.285	0.000	0.025	0.000	0.000	0.000
q_1^4	D/Å^4			−0.174	0.000	−0.022	0.000	0.001	0.000
q_1^5	D/Å^5			0.229	0.000	−0.019	0.000	0.002	0.000
q_1^6	D/Å^6			0.021	0.000	0.027	0.000	0.001	0.000
q_2q_3[b]	D/Å^2			−0.298	0.000				
$q_2q_3^2$[b]	D/Å^3	0.000	0.213	−0.021					
$q_2^2q_3$[b]	D/Å^3	0.000	−0.213	−0.022					
C_z	units	1	cos(θ)	cos(2θ)	cos(3θ)	cos(4θ)	cos(5θ)	cos(6θ)	sin(θ)
q_1	D/Å	−0.456	0.001	−0.046	0.000	−0.005	0.000	0.000	
q_1^2	D/Å^2	−0.788	−0.001	0.095	0.000	−0.006	0.001	0.000	
q_1^3	D/Å^3	0.021	−0.001	0.100	0.000	0.006	0.001	−0.001	
q_1^4	D/Å^4	0.134	0.000	0.002	0.000	0.006	0.000	−0.002	
q_1^5	D/Å^5	0.076	0.000	−0.008	0.000	0.003	0.000	0.000	
q_1^6	D/Å^6	0.037	0.001	−0.084	0.000	0.001	−0.001	0.003	
q_2q_3[b]	D/Å^2	0.370	0.000	0.065					
$q_2q_3^2$[b]	D/Å^3	0.052	0.000						0.030
$q_2^2q_3$[b]	D/Å^3	0.052	0.000						0.029

[a] The dipole moment function is expanded in the CH stretching coordinate as a Taylor series and the torsional coordinate in a Fourier series. The terms that are zero by symmetry have been left out. For the *x* and *z* components, the sin(mθ) diagonal and second order mixed stretching terms are zero. For the *y* component, the cos(mθ) diagonal and second order mixed stretching terms are zero. [b] Fourier expansion is limited (see text).

However, these changes have only a minor effect on the simulated spectral profiles and we have not included them in our model.

The effective coupling constants γ' can be calculated from Wilson G-matrix elements and force constants.[7,16,28] For the methyl groups in 2-, 3-, and 4-methylpyridine, γ' values have been calculated with the HF/6-31G(d) method to be 20.9, 20.5, and 22.0 cm^{-1}, respectively. The γ' values are similar to each other for 2-, 3-, and 4-methylpyridine. The γ' value is expected to change slightly with the torsional angle but this change was not included in our model.

The aim of this study is to contribute to a detailed understanding of methyl torsional effects on the CH stretching overtone spectra through a simulation of the methyl spectral profiles of 2-, 3-, and 4-methylpyridine. The torsional barriers in these three molecules differ in magnitude and symmetry. The results of the simulation are shown in Figures 8−10, where we have compared the observed and simulated spectra for all three molecules from $\Delta v_{CH} = 3-6$. As we have noted, the observed methyl profiles of 3- and 4-methylpyridine are very similar to each other and differ significantly from that of 2-methylpyridine. The simulation has successfully reproduced this feature.

The difference in the methyl profiles between 2-, 3-, and 4-methylpyridine provides strong evidence that torsional modes are actively coupled to the methyl CH stretching overtones. Our simulation is based on the premise that the torsional potentials, stretching frequencies, and anharmonicities of CH oscillators are functions of the torsional angle. This dependence on torsional angle differs among the three methylpyridines. It is this difference along with the change in barrier that leads to the change in methyl profiles between 2-methylpyridine and 3- and 4-methylpyridine. The change does not appear to arise from changes in the dipole moment function. If the 2-methylpyridine spectrum is simulated with the 2-methylpyridine energy parameters and the 4-methylpyridine dipole moment function, the overall results are similar to those in Figure 8.

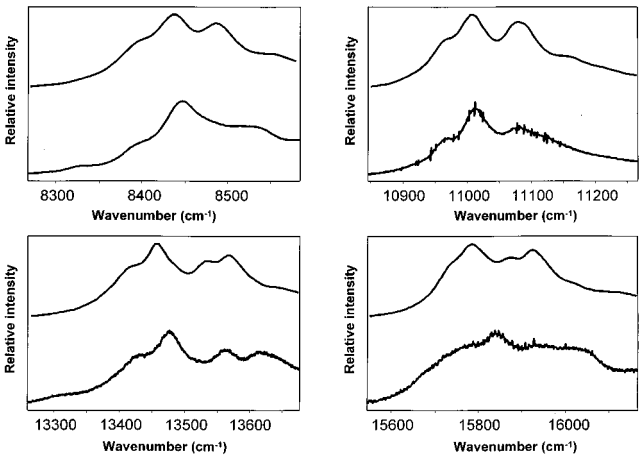

Figure 8. Observed (bottom) and simulated (top) spectra of 2-methylpyridine in the methyl regions of $\Delta v_{CH} = 3-6$.

A "three-peak" characteristic structure is observed in the $\Delta v_{CH} = 4$ and 5 regions of 3- and 4-methylpyridine, which is similar to the corresponding methyl spectral profile of *m*- and *p*-xylene and toluene.[24,25] A comparison of the methyl bands of 3- and 4-methylpyridine at $\Delta v_{CH} = 5$ in Figures 8−10 indicates that the lower energy main peak becomes narrower

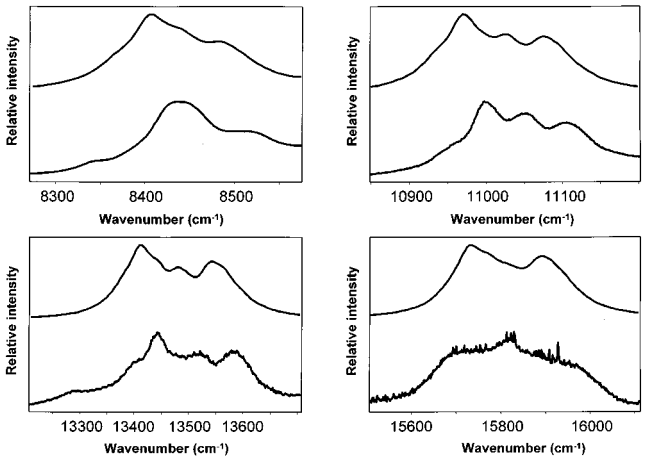

Figure 9. Observed (bottom) and simulated (top) spectra of 3-methylpyridine in the methyl regions of $\Delta v_{CH} = 3-6$.

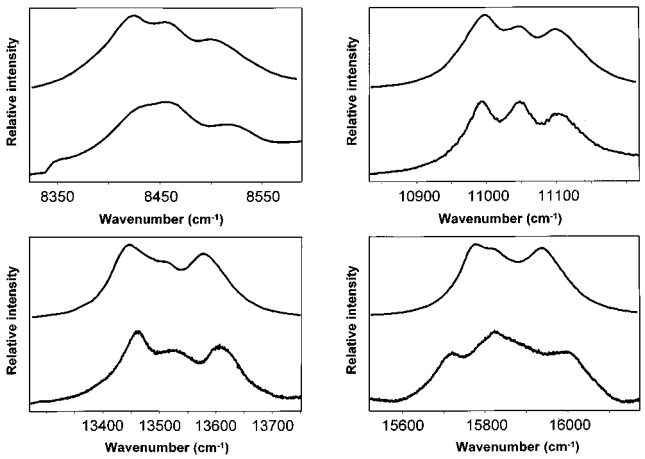

Figure 10. Observed (bottom) and simulated (top) spectra of 4-methylpyridine in the methyl regions of $\Delta v_{CH} = 3-6$.

as the torsional barriers increase. In addition the shoulder that appears on the low-energy side of methyl band profiles at $\Delta v_{CH} = 4$ and 5 becomes stronger as the torsional barriers increase. These features are reproduced in the simulations.

The experimental and ab initio values for the methyl torsional barrier of 2- methylpyridine are 90 and 85 cm^{-1}, respectively.[31] Thus the methyl rotor in 2- methylpyridine is neither a quasi-free rotor, as in *p*-xylene and toluene, nor a conformation preferred rotor, as in *o*-xylene and dimethyl ether.[16,25] The agreement in Figure 8 between the simulated and observed methyl bands in the overtone spectra of 2-methylpyridine confirms that our model is successful for molecules with moderate torsional barriers.

The simulated methyl profiles of 2-, 3-, and 4-methylpyridine in the $\Delta v_{CH} = 6$ region do not correspond to the observed profiles as well as in the $\Delta v_{CH} = 3-5$ regions. The observed spectra have more intensity in the central region at $\Delta v_{CH} = 6$ and wider overall bandwidths than the simulation for all three methylpyridines. These features suggest the existence of greater coupling beyond what is included in our model. The most likely cause for these differences is the existence of a Fermi resonance such as stretching bend interaction. Typically this resonance introduces interactions between states with v quanta of CH stretching and states with $v - 1$ quanta of CH stretching and two quanta of CH bending.

A comparison of the observed and simulated methyl band profiles in Figures 8−10 indicates that both the overall shape of the methyl band and the change of methyl band profiles from molecule to molecule are in good agreement. It is particularly noteworthy that the model gives agreement for 2-methylpyridine, a molecule with an "intermediate size" barrier. This nonadiabatic model can describe successfully spectral manifestations of the interaction between CH stretching and methyl torsion in molecules with complex torsional potentials and dipole moment functions.

Conclusion

We have used a nonadiabatic model to simulate methyl band profiles in the CH stretching overtone spectra in the $\Delta v_{CH} = 3-6$ regions of 2-, 3-, and 4-methylpyridine. The model describes CH stretching with harmonically coupled anharmonic local modes and the methyl torsion with rigid rotors. Variations in the torsional potential, frequency, and anharmonicity with torsional angle are included in the Hamiltonian. A dipole moment function is obtained from ab initio calculations and includes dependence on both the CH stretching coordinates and the methyl torsional angle.

The torsional barrier of methylpyridine increases when methyl substitution gets closer to the nitrogen atom. The methyl band profile of 2-methylpyridine is blue-shifted as compared with the methyl band profiles of 3- and 4-methylpyridine due to the larger mean frequency and smaller mean anharmonicity in the former. The methyl band profile of the overtone spectrum in 2-methylpyridine differs significantly from the methyl band profiles of 3- and 4-methylpyridine. Our results indicate that these differences arise primarily from differences in the change in frequency and anharmonicity with torsional angle, as well as differences in the magnitude of the potential.

We have simulated successfully methyl band profiles of 2-, 3-, and 4-methylpyridine. The torsional potentials of these molecules differ in magnitude, form, and symmetry. Thus, we have developed a model which should have general applicability to a wide class of molecules.

Acknowledgment. We thank Daryl L. Howard for helpful discussions. Z.R. is grateful to the University of Otago for a Specified Research Scholarship. H.G.K. is grateful to CIRES for a visiting faculty fellowship. Funding for this research has been provided by the University of Otago, the Marsden Fund administrated by the Royal Society of New Zealand, and the Natural Science and Engineering Research Council of Canada.

References and Notes

(1) Ellis, J. W. *Phys. Rev.* **1929**, *33*, 27.
(2) Morse, P. M. *Phys. Rev.* **1929**, *34*, 57.
(3) Mecke, R.; Ziegler, R. *Z. Phys.* **1936**, *101*, 405.
(4) Hayward, R. J.; Henry, B. R. *J. Mol. Spectrosc.* **1975**, *57*, 221.
(5) Henry, B. R. *Acc. Chem. Res.* **1977**, *10*, 207.
(6) Watson, I. A.; Henry, B. R.; Ross, I. G. *Spectrochim. Acta A* **1981**, *37*, 857.
(7) Mortensen, O. S.; Henry, B. R.; Mohammadi, M. A. *J. Chem. Phys.* **1981**, *75*, 4800.
(8) Child, M. S.; Lawton, R. T. *Faraday Discuss. Chem. Soc.* **1981**, *71*, 273.
(9) Sage, M. L.; Jortner, J. *Adv. Chem. Phys.* **1981**, *47*, 293.
(10) Henry, B. R. *Acc. Chem. Res.* **1987**, *20*, 429.
(11) Halonen, L. *Adv. Chem. Phys.* **1998**, *104*, 41.
(12) Darling, B. T.; Dennison, D. M. *Phys. Rev.* **1940**, *57*, 128.
(13) Sheppard, N.; Woodman, C. M. *Proc. R. Soc. London, Ser. A* **1969**, *313*, 149.
(14) McKean, D. C. *Chem. Soc. Rev.* **1978**, *7*, 399.
(15) Anastasakos, L.; Wildman, T. A. *J. Chem. Phys.* **1993**, *99*, 9453.
(16) Kjaergaard, H. G.; Henry, B. R.; Tarr, A. W. *J. Chem. Phys.* **1991**, *94*, 5844.
(17) Kjaergaard, H. G.; Yu, H.; Schattka, B. J.; Henry, B. R.; Tarr, A. W. *J. Chem. Phys.* **1990**, *93*, 6239.

(18) Cavagnat, D.; Lespade, L.; Lapouge, C. *J. Chem. Phys.* **1995**, *103*, 10502.
(19) Cavagnat, D.; Lespade, L. *J. Chem. Phys.* **1997**, *106*, 7946.
(20) Cavagnat, D.; Lespade, L. *J. Chem. Phys.* **2001**, *114*, 6030.
(21) Bergeat, A.; Cavagnat, D.; Lapouge, C.; Lespade, L. *J. Phys. Chem. A* **2000**, *104*, 9233.
(22) Lapouge, C.; Cavagnat, D. *J. Phys. Chem. A* **1998**, *102*, 8393.
(23) Zhu, C.; Kjaergaard, H. G.; Henry, B. R. *J. Chem. Phys.* **1997**, *107*, 691.
(24) Kjaergaard, H. G.; Rong, Z.; McAlees, A. J.; Howard, D. L.; Henry, B. R. *J. Phys. Chem. A* **2000**, *104*, 6398.
(25) Rong, Z.; Kjaergaard, H. G., submitted for publication.
(26) Proos, R. J.; Henry, B. R. *J. Phys. Chem. A* **1999**, *103*, 8762.
(27) Atkins, P. W. *Molecular Quantum Mechanics*, 2nd ed.; Oxford University: Oxford, U.K., 1983.
(28) Kjaergaard, H. G.; Henry, B. R. *J. Chem. Phys.* **1992**, *96*, 4841.
(29) MATLAB 6.0 release 12 from MathWorks Inc.
(30) Frisch, M. J.; Trucks, G. W.; Schlegel, H. B.; Gill, P. M. W.; Johnson, B. G.; Robb, M. A.; Cheeseman, J. R.; Keith, T.; Petersson, G. A.; Montgomery, J. A.; Raghavachari, K.; Al-Laham, M. A.; Zakrzewski, V. G.; Ortiz, J. V.; Foresman, J. B.; Cioslowski, J.; Stefanov, B. B.; Nanayakkara, A.; Challacombe, M.; Peng, C. Y.; Ayala, P. Y.; Chen, W.; Wong, M. W.; Andres, J. L.; Replogle, E. S.; Gomperts, R.; Martin, R. L.; Fox, D. J.; Binkley, J. S.; Defrees, D. J.; Baker, J.; Stewart, J. P.; Head-Gordon, M.; Gonzalez, C.; Pople, J. A. *Gaussian 94*, revision D.4; Gaussian, Inc.: Pittsburgh, PA, 1995.
(31) Dreizler, H.; Rudolph, H. D.; Maeder, H. *Z. Naturforsch.* **1970**, *25A*, 25.
(32) Rudolph, H. D.; Dreizler, H.; Seiler, H. *Z. Naturforsch.* **1967**, *22A*, 1738.
(33) Kjaergaard, H. G.; Turnbull, D. M.; Henry, B. R. *J. Phys. Chem. A* **1997**, *101*, 2589.
(34) Scott, A. P.; Radom, L. *J. Phys. Chem.* **1996**, *100*, 16502.
(35) Low, G. R.; Kjaergaard, H. G. *J. Chem. Phys.* **1999**, *110*, 9104.